A GIS GEOMORPHOLOGIC APPROACH FOR DEBRIS RISK ASSESSMENT: AN EXAMPLE IN SICILY (ITALY)

V. Baiocchi [1], L. M. Falconi [2], L. Moretti [2], M. Pollino [3], C. Puglisi [2], G. Righini[2], G. Vegliante[1,4]

[1] DICEA, Sapienza University of Rome, 00184 Rome, Italy (valerio.baiocchi@uniroma1.it)
[2] ENEA, Models and technologies for risks reduction Division, Casaccia and Bologna research centres, Italy
[3] ENEA, Analysis and Protection of Critical Infrastructures Laboratory, Casaccia research centre, 00123 Rome, Italy
[4] Department of Letters and modern Cultures, Sapienza University of Rome, 00161 Rome, Italy

KEY WORDS: Debris flows, Risk analysis, GIS tools, Runout, Peloritani, Giampilieri, Briga, QGIS.

ABSTRACT:

The shallow landslides constitute a consistent current hazard that could increase in the future, especially in the Mediterranean areas. Regional scale hazard maps involving runout estimation are not yet particularly widespread. The study was conducted with the aim of testing a debris flows risk assessment process starting from the runout analysis of a debris flows dataset triggered by the event of October 1, 2009.
Preliminary results highlight how the procedure permit to produce a runout hazard assessment in the valley areas where the more important and vulnerable exposed elements are situated. Despite the obvious limitations, the process appears particularly useful to address the public administration demand for simple tools to manage and direct regional planning.

1. INTRODUCTION

Recent events, including the floods in central Europe in May 2021, have highlighted how climate change is giving rise to scenarios that were neither foreseen nor predictable (Baiocchi et al., 2021). Debris flows are among the natural events most influenced by the climate change due to the close relationship between intense rainfall and debris-flow initiation, widely analysed and documented in literature in several different settings and environments throughout the world (Caine, 1980; Wieczorek & Glade, 2005).
Debris flows, mud flows and debris avalanches are fast moving landslides involving the non-cohesive shallow material lying upon the bedrock, triggered by rainfall infiltration when the soil become saturated (Hungr et al., 2014). These rapid shallow landslides start on neoformation rupture surfaces as small roto-translational slides in the soil over the bedrock and then become mud and debris flows which move downstream with maximum velocity of several meters per second (up to 10 or 15 m/s).
Inducing an increase in extreme precipitation and discharge (IPCC, 2023), climate change seems to can determine debris flows both larger and more frequent. The increase in extreme 1-day precipitation events is likely to have significant impacts on the behaviour of debris flows, especially increasing the magnitude (Stoffel et al, 2014). In mountainous and continental climate areas, the drier conditions in future summers may led to a decrease in sediment supply from hillslopes, which is driven by frost-weathering, and consequently to a reduction in debris-flow occurrence (Hirschberg et al., 2021). Conversely, in temperate and dry climate areas, warming scenarios can mean a significant increase in the number of extreme fire weather events and in these areas post-wildfire extreme rainfall events could be associated to landslides-driven destructive impacts (Touma et al., 2022). Recently burned areas, in fact, have an elevated risk of debris flows, mudslides, and flash floods during rain events due to wildfire-induced changes in soil properties, vegetation loss, and ground cover. In this scenario, the development of practical and affordable methodologies and technologies for debris flow hazard monitoring and assessment constitutes a compulsory aim to achieve the necessary adaptation and mitigation measures.
Debris flows, mud flows and debris avalanches start on steep slopes, usually low anthropized, while the displaced material may be carried downstream also very far from the initiation areas, often invading human settlements, roads or critical infrastructures. Usually, the landslides hazard and risk maps implemented by regional and local authorities mainly include the inventory maps of past landslide and/or landslide susceptibility maps showing only the potential initiation areas, i. e. the areas where landslide failure occurs. Regional hazard maps rarely are the result of debris flows runout analysis and the identification of the propagation areas that may be reached by the displaced material is often missing. To implement simple and reliable analysis processes that addresses both landslides initiation and propagation areas may allow a more exhaustive comprehension of the phenomena, provide more detailed hazard and risk assessment and contribute to strengthen the efficacy of the mitigation measures (Melo & Zezere, 2017).
The study aimed to apply a GIS-based process for the local debris flows risk analysis in two small river basins in the Ionian east side of the Peloritani Mountains (Sicily, Italy). The hazard segments of the risk analysis process leave out the susceptibility analysis, i.e. the identification of the potential initiation areas, focusing on the identification of the debris flows runout and propagation areas.

2. STUDY AREA

The Peloritani Mountain Belt is the southern extremity of the Calabride-Peloritan Arc in the Nord-East Sicily. A SE verging pile of Pre-Alpine metamorphic units nappes composes it, overlapping the sedimentary Maghrebid units (Carbone et al., 2007). Outcropping formations are mainly composed by micashists of various metamorphic grade and secondly by deposition of sedimentary covers. The fast crustal uplifts, starting from upper Pliocene and lower Pleistocene, strongly influenced the overall geomorphology, which resulted in a high energy relief, "V" shaped valleys with steep slopes eroded by torrent-like straight watercourses, narrow and deeply embanked into high rock walls in the mountain sectors, becoming wide and over-flooded in the terminal parts with extensive alluvial fans or dejection cones, ruins of old cliffs, fluvial and marine terraces. The low geomorphologic evolution, typical of a recent uplift, fosters intensive erosion processes and cause a widespread instability along the slopes. The alteration and degradation of crystalline lithotypes, as well as the high erodibility of sedimentary deposits, determine a continuous sediment supply from hillslopes, feeding the soils formation. Brown soils, leptic cambisols and eutric cambisols are present in the area, usually sandy with low clay content (almost 10%) and clearly show tixotrophic characteristics (Napoli et al., 2015). The soil thickness is variable according to the terraces preservation status and its contact with the bedrock varies in depth from 50 to 80 centimetres.

The Ionian side of the Peloritani mountains has experienced considerable urban development since the post-Second World War period (Figure 1). A continuous urban landscape along the coastline, where the population migrated in the past decades leaving the outback original settlements, characterizes the study area. The number of buildings located along the coast has increased significantly over the decades due to the presence of the railway, already present since 1866, and of the Messina-Catania motorway, inaugurated in 1971. Inland and most elevated areas, used in the past for grazing and agriculture, are now covered by woods, shrubs, and meadows, while in the hills and valleys the areas devoted to different agriculture activities prevail. Currently the east coast is characterized by the presence

Figure 1. Comparison between a II World War (Italian Air Force aerial image acquired by the flight of May 24, 1943) and a recent image (Google Earth satellite image, acquired on 09/16/2021).

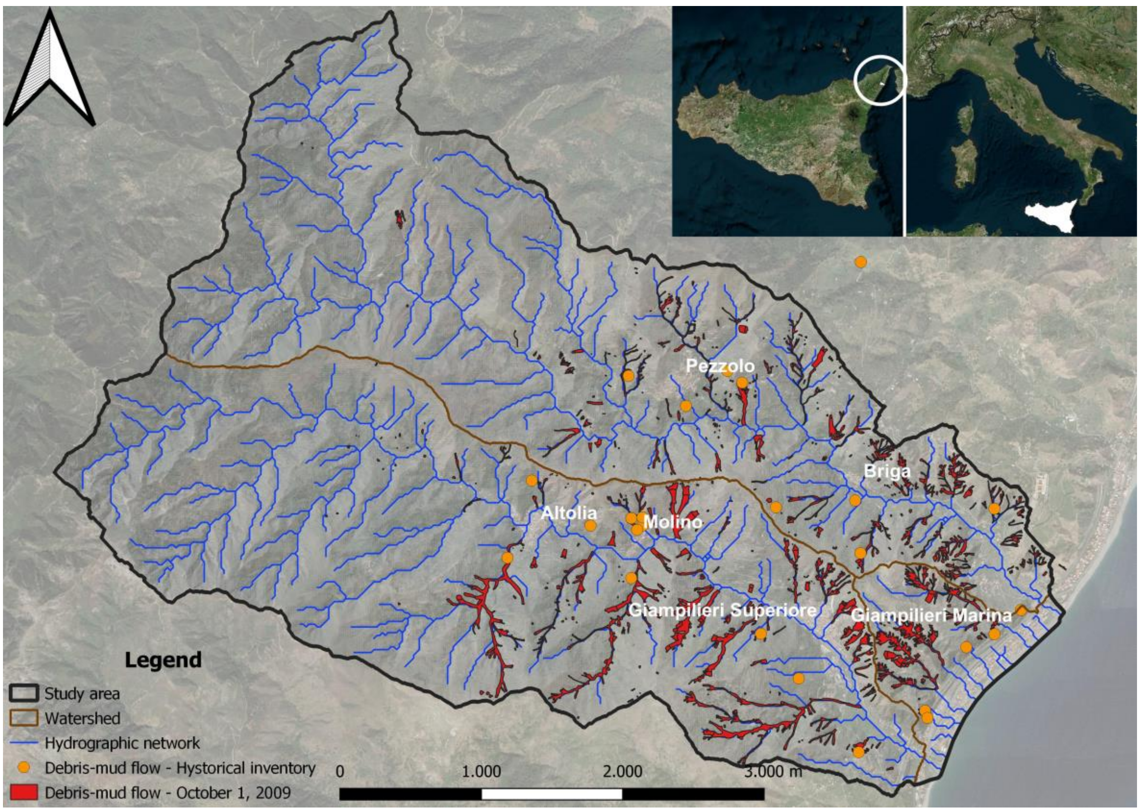

Figure 2. Areas affected by the debris flows of October 1, 2009 (red areas) and past debris flows (orange dots) identified consulting historical documents (Source: ENEA; Elaboration: ENEA).

of an urban continuous and discontinuous fabric, where critical linear infrastructures (roads, motorway, railway, water and gas pipeline, power and communication lines) are located.

The Giampilieri and Briga basins, 15 km south of Messina, extend for 20 km^2 and in recent years have been affected by major landslides events (March 25th, 2007, October 1, 2009, March 1st, 2011). The intense rainfall event of October 1, 2009 determined widespread slope failures and triggering abundant debris and mud flows and debris avalanches (
Figure **2**). The landslides caused severe damages in small villages and along the transportation network in the southern Messina municipalities and in Itala and Scaletta Zanclea areas (
Figure **3** and
Figure 4). In this event that went down in history as the "Messina flood", unfortunately, also many fatalities and injured people were reported.

Landslide hazard in Messina municipality, which experienced also widespread fires in the past, lead often to a generalised high risk due to the specific urbanization and the poor availability of hydro-geomorphologic risk reduction plans.

Figure 3. Effects of the debris flow in the area of S.Stefano di Briga.

Figure 4. Effects of the debris flow in the Altolia village.

3. GEODATABASE AND GIS METHODOLOGY

In the years following the "Messina flood", a well-organized landslide geodatabase has been implemented by ENEA, including landslide inventories and thematic data. The geodatabase was implemented with different GIS software (Arcview, ArcGIS, QGIS) but completely reversed in the last QGIS versions (up to 3.28 – Firenze). It constituted the fundamental tool to produce updated landslide inventory, landslide susceptibility and hazard and risk assessment maps.

The landslide inventory was implemented containing hundreds of rapid shallow landslides triggered by the heavy rains occurred on October 1st, 2009, identified through aerial images observation and field surveys (Falconi et al., 2013; Puglisi et al., 2015).

High scale aerial images, acquired ad hoc after the event of October 1, 2009 by the Civil Protection Department, were used for geomorphological interpretation. A 2 m cell size Digital Terrain Model (DTM; ATA flight 2012-2013), provided by Sicilian Regional Authorities (https://www.sitr.regione.sicilia.it/geoportale/it/Metadata/Details/946), constitutes the basis for the morphometric analysis.

Due to the missing of a detailed soil map, the 1:50,000 geological map of the Messina province (Lentini et al., 2000) was used to spatialize the geotechnical characteristics (friction angle, weight, and cohesion). The fourteen formations outcropping in the study area were distinguished in 6 classes: granular A and B, stratified A and B, massive and crystallin.

A soil thickness map was produced using the GIST model approach (
Figure **5**; Catani et al., 2010), a semi-objective complex process aimed to the definition of the four indices of the equation:

$$h_i = -Kc * C * \eta * \psi^{-1} \quad (1)$$

where h_i represents the soil thickness in each cell of the DTM, Kc is a calibration parameter that adjusts the normalized values of the other indices to real thickness values, C is an index linked to the slope curvature, η is an index linked to the position along the slope profile and ψ is linked to the critical slope threshold. The soil thickness map production is based on the elaboration of the DTM through "r.slope.aspect" and "r.flow" tool", GRASS algorithms available in QGIS, and of the slope values and the lithotechnical characteristics in correspondence with the inventoried debris flows. A 114 field measurements dataset was used to identify the Kc parameter and calibrate the equation.

The Corine Land Cover (CLC) dataset from 1990 to 2018 was acquired constituting the basis for the discretization of the exposed elements. Seventeen different classes were identified among the artificial surfaces (3), the agricultural areas (4) and the forest and seminatural areas (10). Further detailed information was taken from the 2012 Regional Technical Map (1:10,000) of the Sicilian Regional administration, about buildings of public interest and electricity grids, and from Open Street Maps for updates mainly about road network and railway. The QGIS graphic modeler ("Graphic Modeller") was used to execute the algorithms sequences necessary for the estimation of the soil thickness and the calculation of the runout. This definitely powerful tool in GIS processing allowed to create complex models using a simple and easy-to-use interface. The models can be exported in Python language and integrated in the GIS tools libraries of other for Geospatial analysis and Visualization software.

4. HAZARD ANALYSIS

The propagation of the material detached by a rapid shallow landslide is a combination of several causes and elements, extremely difficult to reproduce and analyse in appropriate and exhaustive models. Two main types of procedures are widely used for the runout investigation: empirical-statistical expressions, mainly based on the correlation of geometric parameters, and analytical/numerical models that simulate several parameters of the physical processes (Rickenmann, 2005; Hürlimann, 2008; McDougall, 2014). The extension of the study area and the objective of the investigation usually drive the choice between the two approaches, involving different details, scales and engaged efforts.

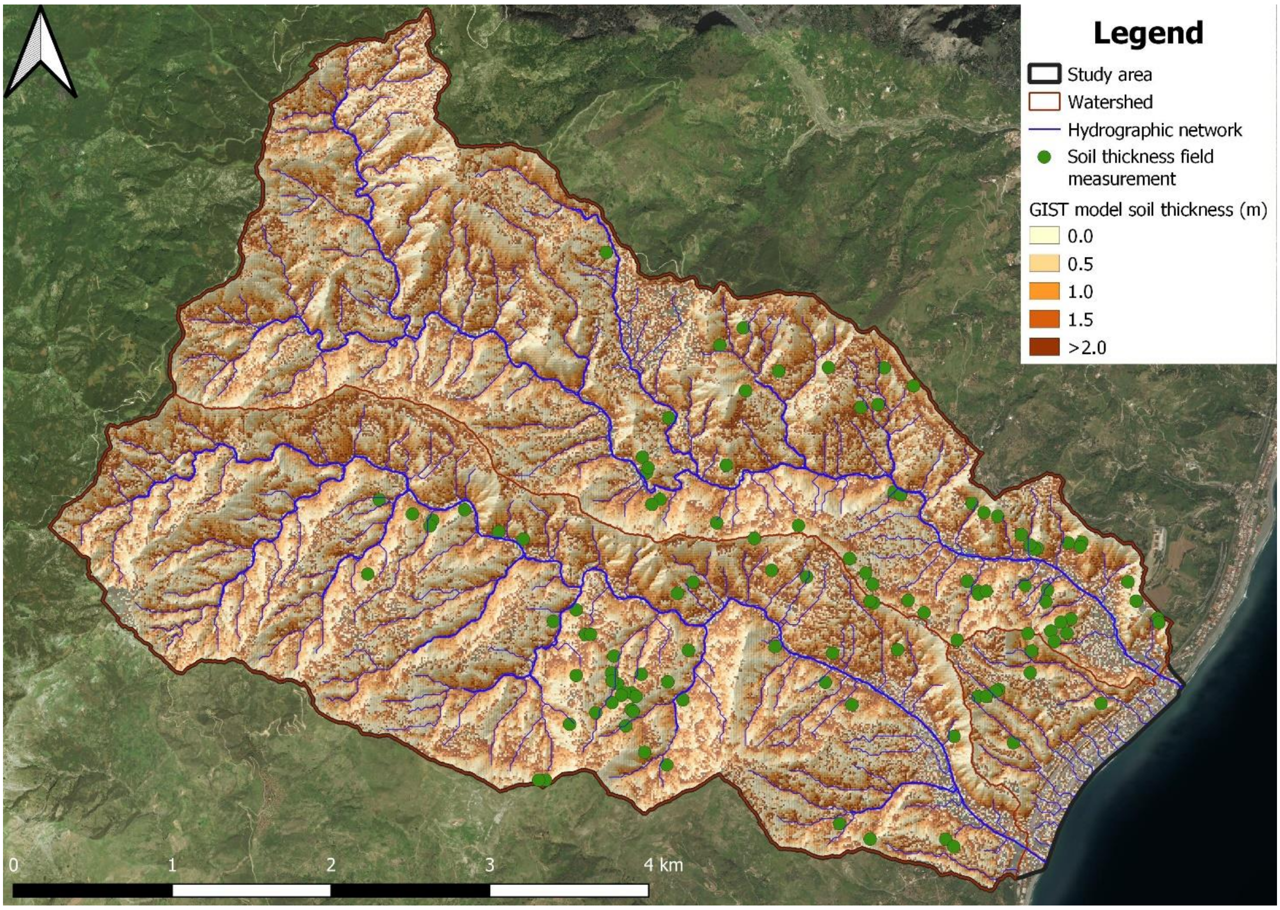

Figure 5. Soil thickness map produced with the GIST model equation with the 2 m cell size DTM. Red areas identify greater soil thickness and green dots indicate the 114 in-field measurements used as calibration points (Source: ENEA; Elaboration: ENEA).

The numerical modelling approach is specifically suitable to characterize a single event at slope scale and to design the slope stabilization works, even if recent studies illustrate some more extended application (Di Napoli et al., 2021).
Empirical/geometric methods rely on simple correlations between some landslide parameters and runout (Jakob & Hungr, 2005). Despite the extreme simplification of the dynamic of the phenomena under investigation, those methods can provide prediction of the extent of the landslide propagation with good reliability (Berti & Simoni, 2007). Moreover, they can successfully support decision-makers and are consistent with more recent guidelines for landslides risk assessment (Corominas et al., 2014).
In this study, the empirical/geometrical approach was applied. The propagation hazard assessment was conducted starting from 100 initiation areas selected randomly from the landslide inventory. The selected dataset was divided in two sub dataset (Figure **6**): 50 initiation areas, with soil thickness field measures located with Garmin GPSMAP 65, were used to calibrate a site-specific runout equation, while the remaining 50 were used as validation dataset. These latter were chosen avoiding those not clearly described in all their components. In fact, the scarp, the initiation area, the path or the toe of the several landslides contained in the inventory are not always evidently shown in the aerial images.
The training landslides dataset were analysed to apply the Legros (2002) runout equation:

$$L = aV^b \tag{2}$$

where L is the runout distance and V is the volume of the initiation area. Through a regression analysis of runout distance and the volume (R2 = 0.7524), the a and b site-specific parameters were defined (Falconi et al., 2023; Figure 7).

Subsequently, three distinct GIS tools were applied to the validation dataset of landslides, implemented using several algorithms available in the processing instruments library of QGIS. Basing on the DTM elaboration, the first tool produced a new linear layer consisting in the water drop path, i.e. the path that a drop of water would take across the land surface.

Applying the site-specific parameters of the Legros equation, the second tool cuts each line of the drop water path layer at the specific estimated runout distance. Once the runout path of each potential landslide was drawn, the third tool assigns a velocity distribution along the paths. Implementing the tool, the propagation dynamics were greatly simplified by making several necessary approximations. Among the main ones, there are the standardization of the propagation process of all potential landslides and the imposition of a linear variation in the velocity distribution, in both acceleration and deceleration phases.

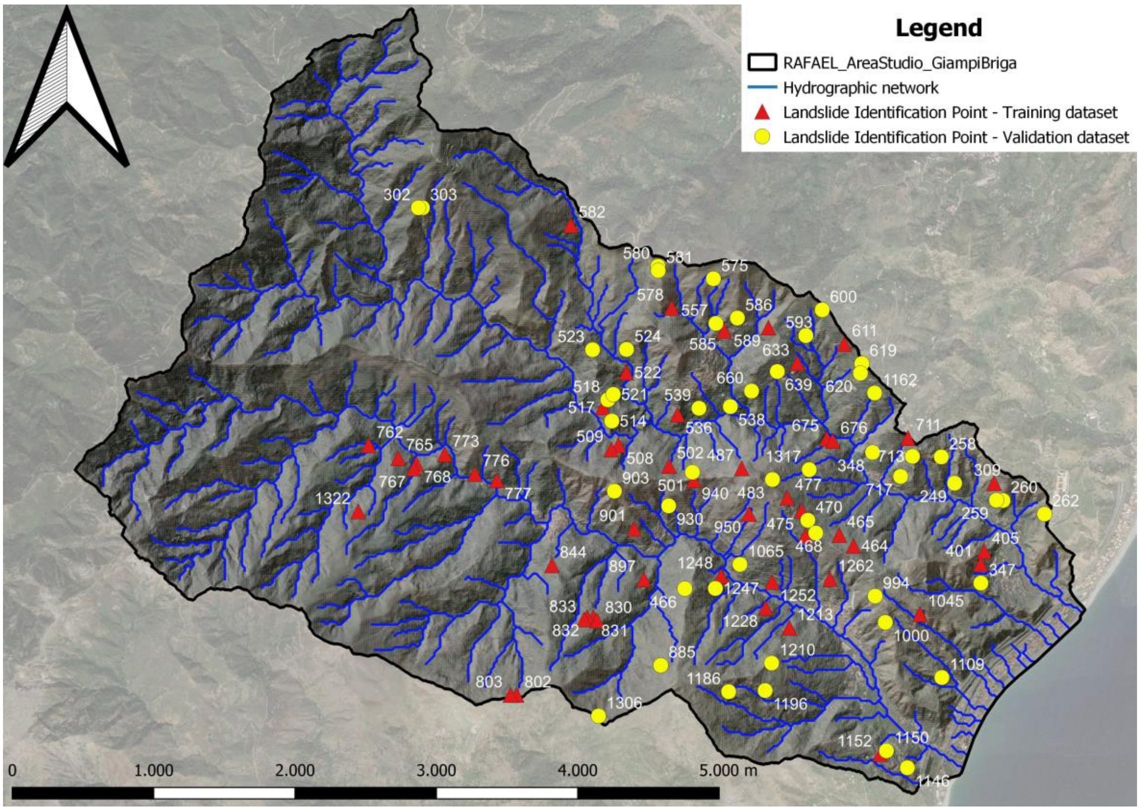

Figure 6. Study area with the 100 observed Landslide Identification Points distinguished in training (red triangle) and validation (yellow dot) dataset (Source: ENEA; Elaboration: ENEA).

Basing on field measurements, the tool assumes that, starting from 0 m/s in the higher point of the main scarp (Landslide Initiation Point), the mobilized masses accelerate up to the point of peak velocity (8.4 m/s), reached at one quarter of the path, and then decelerate. Assuming as constant the volume along the path and homogenous the rheologic characteristic of the mobilized masses, in particular the density (δ = 2,000 kg/m^3), the impact force of each potential rapid shallow landslides was estimated as proportional to the kinetic energy discretized in four classes.

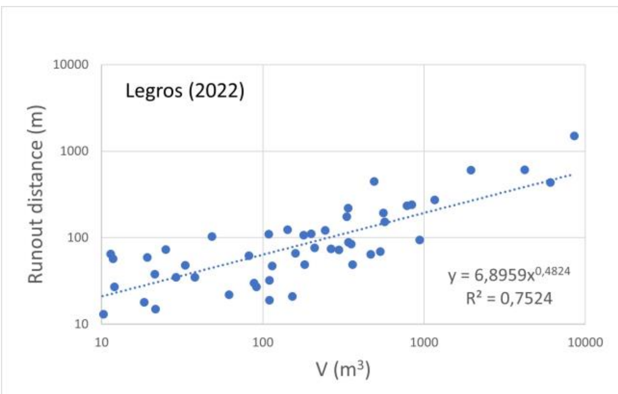

Figure 7. Regression calculated using observed runout distance (y axis) and estimated volume values (x axis) of the training dataset.

A 10 meters buffer of the drawn path of each debris flows was produced, attributing to the different twenty sectors of the polygons of each landslide path a different impact force. Consequently, the analysed territory was discretised by distinguishing areas with different susceptibility to be reached by the mobilized material with different destructive capacity (Figure 8).

5. EXPOSURE ANALYSIS

The exposure analysis is aimed to attribute a value to all kind of elements typology present in a territory, exposed to a certain hazard and therefore subject to potential losses. The types of elements exposed to a natural hazard are population, structures and infrastructures, properties, economic activities, public services and any other value present in a given area subject to a risk analysis (Van Westen, 2011).

Integrating CLC and other available data, sixteen different types of exposed elements were identified: continuous and discontinuous urban fabric, four typology of public interest buildings (schools, churches, cemeteries, other community buildings), cultivated areas, wooded areas, pastures and shrubs, tracks, roads, motorway, railway, gas station, power lines and communication tower (Figure 9). A relative value from 1 to 4 (lower to higher importance) was assigned to each class of exposed elements based on qualitative evaluations about social and economic importance (Table 1).

6. VULNERABILITY ANALYSIS

Vulnerability is defined as "the conditions determined by physical, social, economic and environmental factors that increase the susceptibility of a community to the impact of

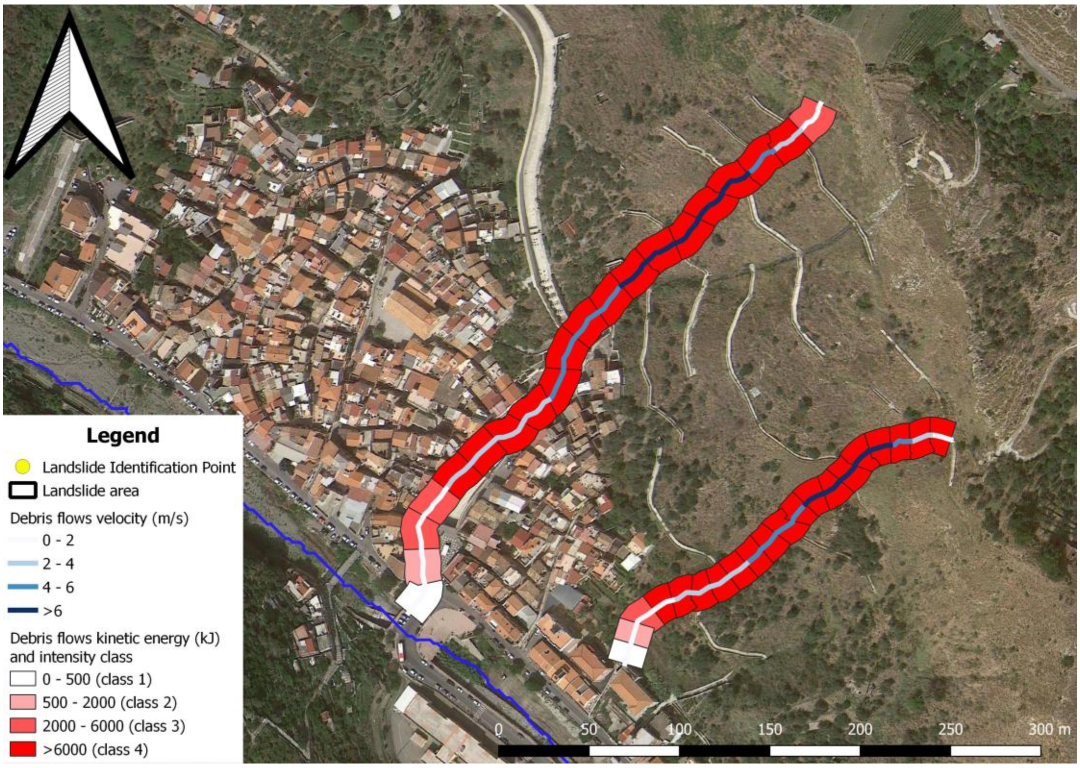

Figure 8. Debris flows hazard assessment for two initiation areas of the Giampilieri village. The lines starting from the higher point of the scarp of each debris flow (yellow dot) were used to visualize the velocity distribution (from white to blue) and the different kinetic energy (from white to red) along the paths (Source: ENEA; Elaboration: ENEA).

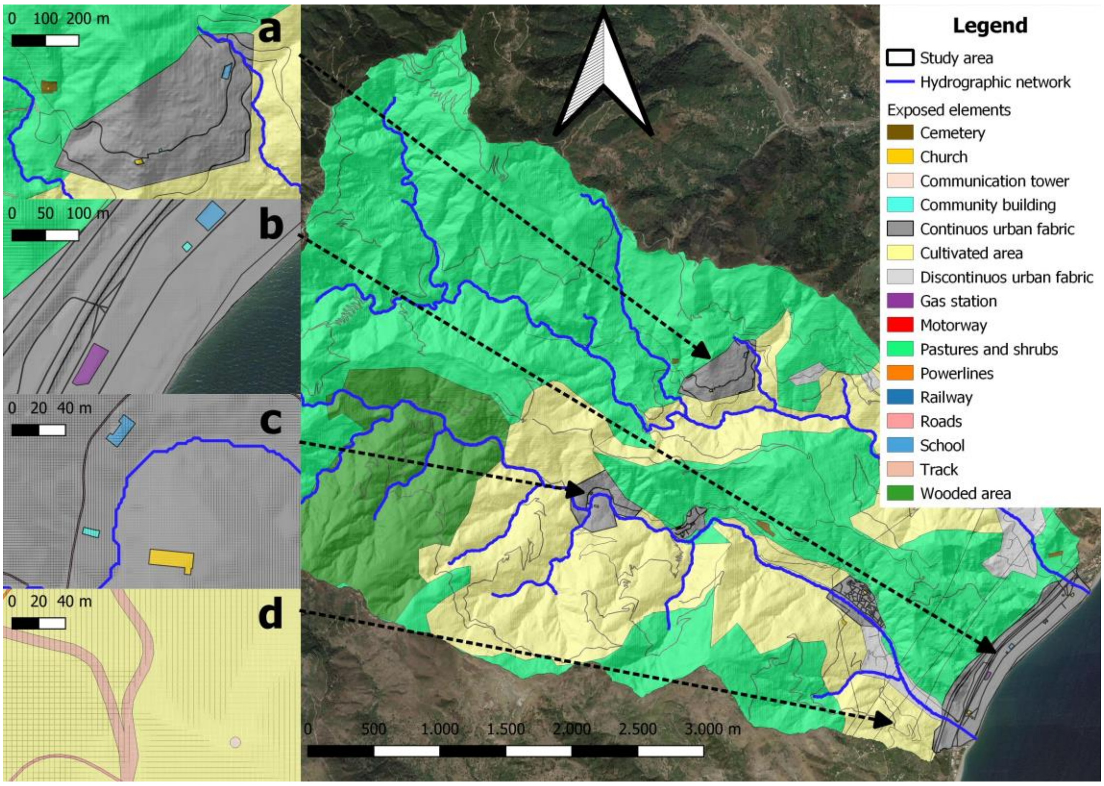

Figure 9. Exposed elements map with four focusing detailed areas: a) Pezzolo village; b) gas station, school and a community building in the Giampilieri Marina village; c) the center of Altolia village; d) a communication tower over Giampilieri Marina village (Source: ENEA; Elaboration: ENEA).

hazards". It is identified as the degree of loss of one or more elements subject to a natural event having a certain magnitude and generally expressed on a scale from 0 to 1, respectively "no damage" and "total loss" (Fell, 1994). For people, vulnerability corresponds to the probability that a natural event could cause victims. Among the methods used to analyse vulnerability there are empirical ones, in which discrete values are usually provided for a range of landslide intensity (Cardinali et al., 2002). In this study a different degree of relative vulnerability from 1 to 4 (lower to higher vulnerability) was attributed to the exposed elements based on the different expected response of each class to the stresses induced by the debris flows phenomena with different intensities (
Table **1**). Among others, the following considerations guided the attribution of vulnerability values:

- buildings of public importance (i. e. schools) and discontinuous urban fabric are supposed to have more solid construction characteristics than buildings in historical centres and churches, as well as in the more ancient villages that constitute the continuous urban fabric;
- viaducts and tunnels make motorways less vulnerable than ordinary roads and railways.

Typology	Exposure	Vulnerability
Pastures and shrubs	1	1
Wooded areas	1	2
Tracks	1	3
Roads	2	3
Cultivated areas	2	4
Motorway	3	2
Discontinuous urban fabric	3	3
Gas station	3	3
Railway	3	4
Cemeteries	3	4
Communication tower	3	4
Power lines	3	4
Schools	4	3
Other community buildings	4	3
Continuous urban fabric	4	4
Churches	4	4

Table 1. Matrix with exposure and vulnerability values assigned to each typology of the exposed elements.

https://doi.org/10.5194/isprs-archives-XLVIII-1-W1-2023-33-2023

7. RESULTS

A comparison between observed and estimated runout values using the site-specific equation allowed to evaluate the performance of the used equation (Figure 10). The statistical measurement (R^2 = 0.7369) expresses a good forecasting capacity taking into account however that the estimated runout distances can vary between 0.5 and 2 times of the observed debris flows path.
The dimensions of the observed landslides vary largely in terms of geometric and kinematic parameters with differences exceedingly even one or two orders of magnitude for area, volume and speed (Table 2).
The discretization of the study area in terms of risk value followed the classic risk equation:

$$R = H*E*V \tag{3}$$

where R is the risk value and H, E and V area respectively the hazard, exposed elements and vulnerability values.
The values of E and V (
Table **1**) were multiplied by the value of the intensity class (
Figure **8**) all divided into classes from 1 to 4. The set of values (from 1 to 64) was further divided into 4 homogeneous classes by attributing the value 0 to the portions of territory not affected by landslides.
Preliminary results show that the higher risk level areas are concentrated in the continuous urban fabric areas where the more important and vulnerable exposed elements are situated. This aspect is clearly evident in the case of the two debris flows that insist on the Giampilieri village (Figure 11). Further improvements will focus on the consolidation of the analysis process and on the application of the methodology to other areas prone to debris flows.

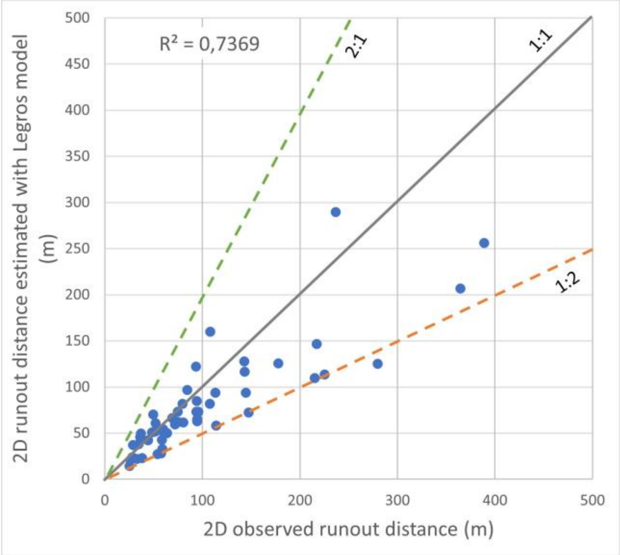

Figure 10. Comparison between observed and estimated 2D runout distances calculated for the validation dataset with Puglisi et al. (2015) equation.

Landslides features	Area (m^2)	Volume (m^3)	Velocity (m/s)	Kinetic energy (kJ)
Min	29	5	0	0
Med	613	401	4	5294
Max	4216	2317	8	163473

Table 2. Characteristics of the fifty observed initiation areas (area and volume) and of the runout path segments (velocity and energy).

8. CONCLUSIONS

The shallow landslides constitute a consistent current hazard that could increase in the future, especially in the Mediterranean areas. Regional scale hazard maps involving runout estimation are not yet particularly widespread. The study was conducted with the aim of testing a debris flows risk assessment process starting from the runout analysis of a debris flows dataset triggered by the event of October 1, 2009. The runout analysis

https://doi.org/10.5194/isprs-archives-XLVIII-1-W1-2023-33-2023 | © Author(s) 2023. CC BY 4.0 License.

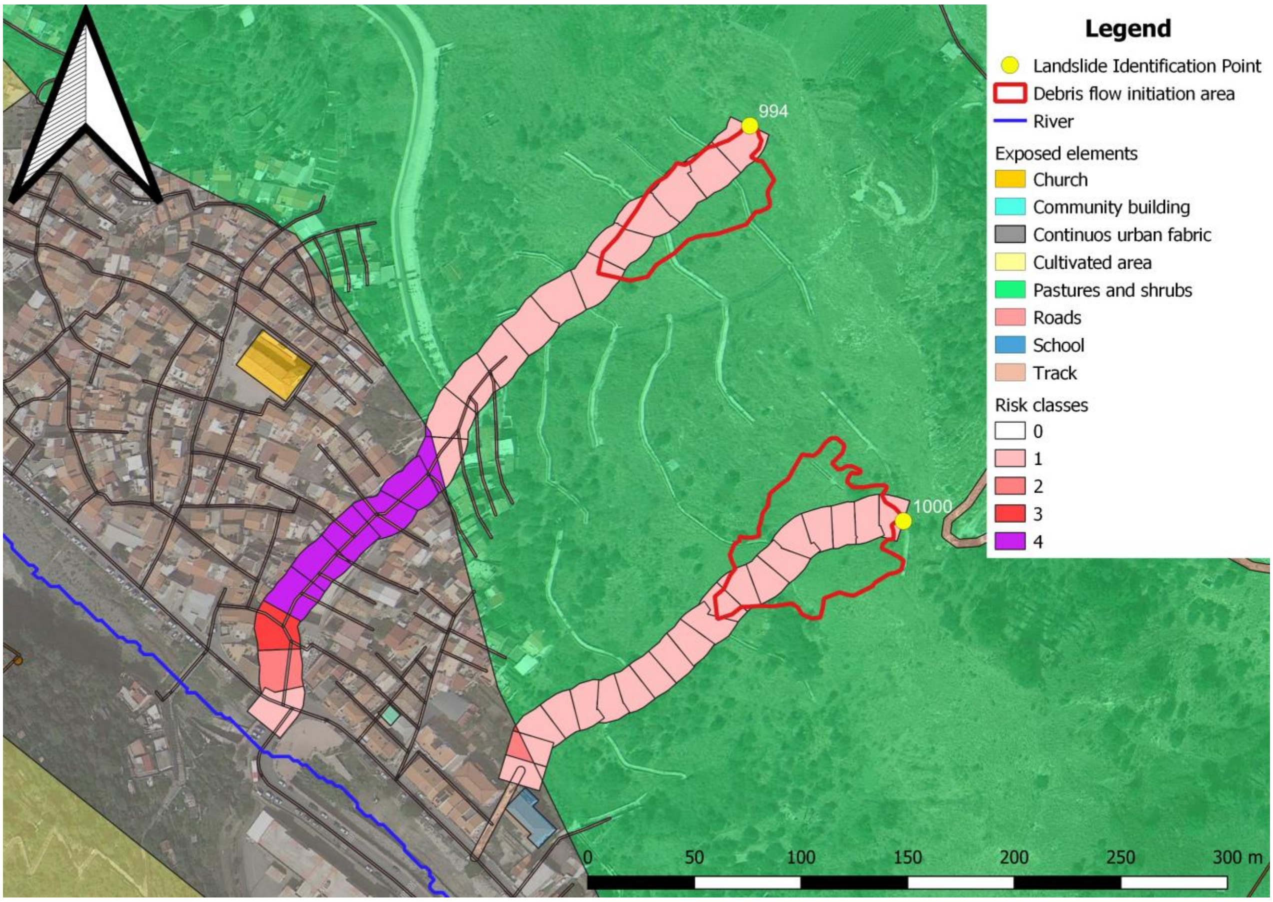

Figure 11. Debris flows risk assessment for the two evaluated debris flows insisting on the Giampilieri village area (Source: ENEA; Elaboration: ENEA)

process applied in this study uses initiation areas as starting data. Since these are the typical output of the common landslide susceptibility analysis, the approach constitutes the second segment of a complete hazard analysis process at regional scale.
Although the runout distances calculated with the Legros (2000) equation present a certain level of approximation, the estimate allows reasoning in quantitative terms on the hazard level in the areas downstream of the initiation areas. Whether specific GIS tools for automated runout estimation will be refined, more complex but more effective functions could also be used (Falconi et al., 2023).
The specific runout toolset, implemented with QGIS, largely facilitated the runout analysis that required the execution of numerous algorithms in sequence to achieve the identification of the landslide path and the runout distance from several potential initiation areas. The automatic execution of a chain of operations into a single process, provided the opportunity of save time and effort in the GIS analysis and made the specific implemented tools well suited for being integrated in landslide early warning systems.
Through a qualitative risk evaluation matrix, the analysis allowed to discretize a territory in qualitative different classes. The approximations introduced in the estimation of volumes, speeds and consequently of energy and in the distribution of energy along the path make the process as no more than a preliminary approach. The exposure and vulnerability values used in the study are exclusively instrumental to implement the process. More in-depth analyses on the exposed elements values are in the responsibility of public administrations as well as their vulnerability must be an object of interest for structural engineering.
Despite the obvious limitations, the process appears particularly useful to address the public administration demand for simple tools to manage and direct regional planning. Further investigations will hopefully contribute to fill the gap currently present in the definition of debris flow hazard maps. Due to the use of public datasets, it can be exported successfully to other context and Countries where decision-makers are committed in landslides risk assessment.

ACKNOWLEDGEMENTS

This study was carried out as part of the RAFAEL project co-financed by the Ministry of University and Research under the PON “Research and Innovation” 2014–2020 and FSC funds referred to the D.D. of 13 July 2017 n. 1735—Application ARS01_00305 “Smart Secure and Inclusive Communities” specialization area.
The DTM is owned by the Sicilian Region, provided on 11/29/2022 to n° 2022-S-3418.

REFERENCES

Baiocchi, V., Vatore, F., Lombardi, M., Monti, F., Onori, R., 2021. The contribution of open-source gis software and open spatial data for the re-evaluation of landslide risk and hazard in view of climate change. *Geographia Technica*, 16 (Special

Issue), pp. 153 – 162. https://doi.org/10.21163/GT_2021.163.12

Berti, M., Simoni, A. 2007. Prediction of debris flow inundation areas using empirical mobility relationships. Geomorphology, 90,144–161

Caine, N. 1980. The rainfall intensity: duration control of shallow landslides and debris flows. Geogr Ann Ser Phys Geogr 62, 23. https://doi.org/10.2307/520449

Carbone, S., Messina, A., Lentini, F. 2007. Note illustrative della carta geologica d'Italia alla scala 1:50.000, Foglio 601 - MESSINA-REGGIO DI CALABRIA. S.EL.CA. s.r.l., Firenze

Cardinali, M., Reichenbach, P., Guzzetti, F., Ardizzone, F., Antonini, G., Galli, M., Cacciano, M., Castellani, M., Salvati, P., 2002. A geomorphological approach to the estimation of landslide hazards and risks in Umbria, Central Italy, in Natural Hazards and Earth System Sciences, 2, European Geophysical Society, 2002, pagg. 57-72

Catani, F., Segoni, S., Falorni, G. 2010. An empirical geomorphology-based approach to the spatial prediction of soil thickness at catchment scale WATER RESOURCES RESEARCH, VOL. 46, W05508, https://doi.org/10.1029/2008WR007450, 2010

Corominas, J., van Westen, C., Frattini, P., Cascini, L., Malet, J.P., Fotopoulou, S., Catani, F., Van Den Eeckhaut, M., Mavrouli, O., 2014. Recommendations for the quantitative analysis of landslide risk. Bulletin of Engineering Geology and the Environment, 73(2): 209–263. https://doi.org/10.1007/s10064-013-0538-8

Di Napoli, M., Di Martire, D., Bausilio, G., Calcaterra, D., Confuorto, P., Firpo, M., Pepe, G., Cevasco, A. 2021. Rainfall-Induced Shallow Landslide Detachment, Transit and Runout Susceptibility Mapping by Integrating Machine Learning Techniques and GIS-Based Approaches. Water 2021, 13, 488. https://doi.org/10.3390/w13040488

Falconi, L. M., Moretti, L., Puglisi, C., Righini G., 2023. Debris and mud-flows runout assessment: a comparison among empirical geometric equations in the Giampilieri and Briga basins (east Sicily, Italy) affected by the event of 1st October 2009. Natural Hazards https://doi.org/10.1007/s11069-023-05945-8

Falconi, L. M., Campolo D., Leoni G., Lumaca S., Puglisi C., 2013. Geomorphology hazard assessment of Giampilieri and Briga river basins after the rainfall event on the October 1, 2009 (Sicily, Italy). *Landslide Science and Practice*, Volume 1: Landslide Inventory and Susceptibility and Hazard Zoning. Springer-Verlag Berlin Heidelberg, ISBN: 978-3-642-31325-7, pp. 533-540

Fell, R. 1994. Landslide risk assessment and acceptable risk. Canadian Geotchnical Journal, 31, Canada 1994, pagg. 261-272

Hirschberg, J., Fatichi, S., Bennett, G.L., McArdell, B. W., Peleg, N., Lane, S. N., 2021. Climate change impacts on sediment yield and debris-flow activity in an Alpine catchment. *Journal of Geophysical Research: Earth Surface*, *126*, e2020JF005739. https://doi.org/10.1029/2020JF005739

Hungr, O., Leroueil, S., Picarelli, L., 2014. The Varnes classification of landslide types, an update Landslides, 11: 167–194. doi:10.1007/s10346-013-0436-y

Hürlimann, M., McArdell, B. W., Rickli, C., 2015. Field and laboratory analysis of the runout characteristics of hillslope debris flows in Switzerland. Geomorphology, 232, 20-32. https://doi.org/10.1016/j.geomorph.2014.11.030

IPCC, 2023. Climate Change 2023: Synthesis Report of The IPCC Sixth Assessment Report (AR6) IPCC – Switzerland - https://www.ipcc.ch/report/sixth-assessment-report-cycle/

Jakob, M., Hungr, O., 2005. Debris-flow hazard and related phenomena. New York, Springer

Lentini, F., Catalano, S., Caliri, A., Carbone, S., Carveni, P., Di Stefano, A., Gargano, C., Grasso, M., Guarnieri, P., La Manna, F., Lentini, R., Messina, A., Romeo, M., Strazzulla, S., Vinci, G., Vinciguerra, G.,. 2000. Carta geologica della Provincia di Messina (Sicilia nord-orientale) e Note illustrative, scala 1:50.000. S.EL.C.A. Editore

Melo, R., Zezere,, J. L., 2017. Debris-flow failure and run-out susceptibility assessment in the Zêzere river basin (Serra da Estrela, Portugal). Revista Brasileira de Geomorfologia v. 18, nº 1 (2017). http://dx.doi.org/10.20502/rbg.v18i1.985

Mc Dougall, S., 2014. Canadian Geotechnical Colloquium: Landslide runout analysis: current practice and challenges. Can. Geotech. J. 54: 605–620 (2017) dx.doi.org/10.1139/cgj-2016-0104. https://cdnsciencepub.com/doi/10.1139/cgj-2016-0104

Napoli, R., Crovato, C., Falconi, L. M., Gioè, C., 2015 Soil water content and triggering of debris flows in the Messina area (Italy): preliminary remarks. Engineering Geology for Society and Territory - Volume 2, *Landslide Processes*. Springer International Publishing Switzerland, ISBN: 978-3-319-09057-3, pp 2113–2117

Puglisi, C., Falconi, L. M., Gioè, C., Leoni, G., 2015. Contribution to the runout evaluation of potential debris flows in Peloritani Mountains (Messina, Italy). Engineering Geology for Society and Territory - Volume 2, *Landslide Processes*. Springer International Publishing Switzerland, ISBN: 978-3-319-09057-3, pp. 509-513

Rickenmann, D., 2005. Runout prediction methods. In: Jakob, M., Hungr, O. (Eds.), Debris-flow Hazards and Related Phenomena. Springer, Berlin, pp. 305–324

Stoffel, M., Mendlik, T., Schneuwly-Bollschweiler, M., Gobiet, A. (2014). Possible impacts of climate change on debris-flow activity in the Swiss Alps. Climatic Change (2014) 122:141–155. DOI 10.1007/s10584-013-0993-z

Touma, D., Stevenson, S., Swain, D. L., Singh, D., Kalashnikov, D. A., Huang, X., 2022. Climate change increases risk of extreme rainfall following wildfire in the western United States. *Science Advances*, 8 (13), eabm0320. https://www.science.org/doi/10.1126/sciadv.abm0320

Van Westen, C. J., Alkema, D., Damen, M. C. J., Kerle, N., Kingma, N.C., 2011. *Multi-hazard risk assessment. Distance education course. Guide book.*, United Nations University – ITC School on Disaster Geoinformation Management (UNU-ITC DGIM), 2011

Wieczorek, G.F., Glade, T., 2005. Climatic factors influencing occurrence of debris flows. In: Jakob M, Hungr O (eds) Debris-flow hazards and related phenomena, pp 325–362